

Comparison of Formability between Commercially Pure Titanium JIS Class 1 Sheet and Steel Sheets and Forming Simulation Technology

Ryotaro MIYOSHI*

Yoshiaki ITAMI

Abstract

To understand the formability of commercially pure titanium JIS class 1 sheet, we conducted various tests with steel sheets for deep drawing having the same level of strength and SUS316. The results of the tensile test show that titanium has higher anisotropy than the steel sheet and SUS, and has almost the same level of strength and ductility as the steel sheet but has lower ductility than the SUS. Also, titanium has the largest r value while the SUS has the smallest one. The results of the punch stretch forming test with various blanks show that the limiting dome height of titanium is equal to or greater than that of the steel sheet, and depending on the blank shape, titanium has a larger stretching height than the SUS. At the deep drawing test, the limiting drawing ratios (LDR) of the SUS, steel sheet, and titanium are 2.2, 2.3, and 2.6, respectively and titanium had large ears formed in a direction different than that estimated based on Δr . With Hill's quadratic orthotropic yield function, we performed square deep drawing simulation for the titanium, where the same plate thickness distribution was obtained. In the future, we will develop a constitutive law that takes into account anisotropic hardening, aiming for further improvement in accuracy.

1. Introduction

Titanium is the ninth most abundant element that exists in the earth crust. However, since it is difficult to refine, it has a short history of usage of only a few decades since the start of its industrial use. However, by taking advantage of its features of light weight, high strength, high corrosion resistance, ease of developing various colorings, and excellent designability, titanium has expanded its application range,¹⁾ and in recent years, has come to be recognized widely as one of the general metals. On the other hand, the strong impression that titanium is light and strong and the image of low ductility associated with its hexagonal close-packed structure (hcp) form an image of titanium being a material difficult to form. In fact, titanium has an excellent balance of strength and ductility, and in the representative field of application such as of plate type heat exchanging machines, automobiles, building materials, and high-end consumer products, commercially pure titanium JIS class 1 that underwent severe press forming is used. Hereafter, in order to expand

the application of titanium in the market that requires such a high degree of forming, firstly it is important for the pure titanium with a central focus on JIS class 1 to be widely recognized as a material having good formability. Furthermore, in order to make the most of the formability, it is necessary to expand the methods for solving problems such as of strong anisotropy caused by hcp, difficulty in the simulation calculation therefor,^{2,3)} and high friction coefficient. This article reports the results of the tensile test, hemi spherical punch stretching test, and the cylindrical cup drawing test conducted to acquire data to intuitively understand the high formability and the anisotropy of commercially pure titanium JIS class 1 by comparing with the results of the tests conducted for the deep drawing steel sheets for automobile use and the general purpose stainless steel SUS316. Furthermore, an example of our efforts to improve the accuracy of the simulation calculation by adding the factor of titanium anisotropy is introduced.

* Researcher, Titanium & Stainless-steel Research Dept., Materials Reliability Research Lab., Steel Research Laboratories
20-1 Shintomi, Futttsu City, Chiba Pref. 293-8511

2. Experiment Method

2.1 Test material

For the tests, the following materials were used: commercially pure titanium JIS class 1 sheet of 0.49 mm thickness for the press forming use (hereinafter referred to as CP-Ti) having the chemical compositions as shown in Table 1, deep drawing steel sheet for automobile use JAC270D of 0.50 mm thickness (hereinafter referred to as LC-Steel), and the general purpose stainless steel SUS316 sheet of 0.54 mm thickness (hereinafter referred to as SUS316), having the chemical compositions as shown in Table 2. Figure 1 shows the microstructure of each test material. The CP-Ti microstructure is equiaxed, has an average grain size of about 60 μm, and the slight twin was formed by the strain developed in a tension leveler. The microstructures of LC-Steel and SUS316 are equiaxed, and are about 10–15 μm.

2.2 Tensile test, hemi spherical punch stretching test, and cylindrical cup drawing test, and method of strain analysis

As for each test material, the tensile test, hemi spherical punch stretching test, and cylindrical cup drawing test were conducted. The hydraulic bulge test was also conducted for LC-Steel. For the tensile test, JIS13B test pieces (gauge length 50 mm) were prepared, taken from the rolling direction (hereinafter referred to as the L direction), 45° direction (hereinafter referred to as the D direction), and the rolling width direction (hereinafter referred to as the T direction). The strain rate was set at 0.3 %/min until 0.2% proof stress was reached, and then after, set at 30 %/min. Also, the r-value at the 4% nominal strain was measured. In the hemi spherical punch stretching test, to vary the strain mode, the blank shape was changed: 30L×90T mm, 40L×90T mm, 50L×90T mm, 60L×90T mm, 70L×90T mm, 90L×90T mm, 90L×70T mm, 90L×60T mm, 90L×50T mm, 90L×40T mm, and 90L×30T mm. In the square 90L×90T mm blank, equibiaxial strain deformation occurs, and in other rectangular blanks, the main strain occurs in the long axis direction. The shorter the short axis length, the smaller the strain in the short axis direction becomes.⁴⁾ For the dies, a spherical punch of φ40 mm and a die was formed draw bead with r6 mm for 2 mm clearance were used. To provide a uniform coefficient of friction to all materials, NAFLON tape TOMBO 9001 t 0.05 mm (hereinafter

referred to as NAFLON tape) was used for lubrication. The blank holding load was 7 tons, the punch climb rate was set at 20 mm/min, and the limiting dome height of each blank was evaluated. In the hydraulic bulge test, a 150L×150T mm blank was used. A die was formed draw bead with a hole diameter of φ100 mm, r10 mm was used. The blank holding load was 40 tons, and the hydraulic pressure was increased gradually so that the blank became fractured after about 5 min. For the cylindrical cup drawing test, circular blanks with 4 mm pitch diameter increments between φ80–108 mm were prepared. For the dies, a cylindrical punch of φ40 mm, r8 mm and a die with 1.75 mm clearance and r10 mm were used. To provide a uniform coefficient of friction to all materials, NAFLON tape was used for lubrication. The blank holding pressure was set at 4 MPa, the punch climb rate was set at 20 mm/min, and the limiting drawing ratio (hereinafter referred to as LDR) was measured. For the recognition of the strain after test, 2 mm square grid marking was previously provided to each test piece. The strain in the vicinity of the fracture location in the tensile test, hemi spherical punch stretching test, and the hydraulic bulging test was measured by a noncontact type strain analysis apparatus AutoGrid, and the forming limit diagram (FLD) was developed.

3. Result of Experiment and Consideration

3.1 Tensile test

Table 3 shows the result of the tensile test. As compared with the results of LC-Steel and SUS316, the anisotropy of CP-Ti is very large, the 0.2% proof stress grows higher in the order of the L<D<T direction, and the tensile strength grows higher in the order of D<L<T. Furthermore, the uniform elongation (U-EL) and the total elongation (T-EL) show an adverse trend of T<L<D. The r-value becomes higher in the order of the L<D<T direction. The value in the T direction was remarkably high at 7.9. When the average values in the L, D, and T directions of the materials are compared, regarding the total elongation and the tensile strength, CP-Ti≈LC-Steel<SUS316, and as for the r-value, SUS316<LC-Steel<CP-Ti. In addition, the anisotropy of the r-value was evaluated by the in-plane anisotropy Δr of Expression (1).

$$\Delta r = \frac{(r_L + r_T)}{2} - r_D \tag{1}$$

where r_L, r_T, and r_D respectively represent the r-value in the L, T, and D direction, respectively. Δr is 0.5 in CP-Ti, 0.0 in LC-Steel, and -0.1 in SUS316.

Figure 2 shows the nominal stress-nominal strain diagram (here-

Table 1 Chemical composition of CP-Ti (mass%)

Material	N	C	O	Fe	Ti
CP-Ti	0.001	0.005	0.5	0.03	Bal.

Table 2 Chemical composition of LC-Steel, SUS316 (mass%)

Material	C	Si	Mn	P	S	Ni	Cr	Mo	Fe
LC-Steel	0.004	0.005	0.079	0.019	0.0039	–	–	–	Bal.
SUS316	0.016	0.59	1.31	0.033	0.0086	10.57	16.91	2.01	Bal.

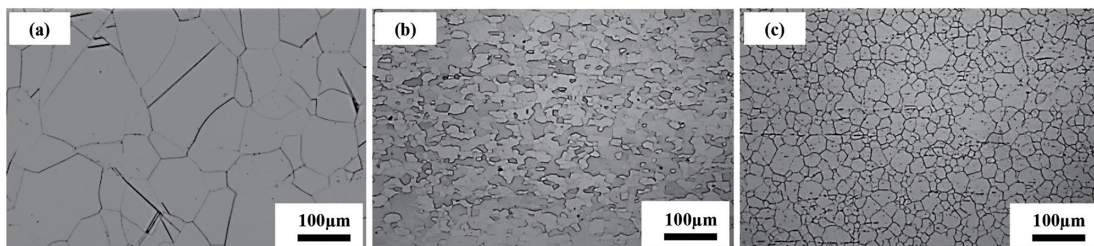


Fig. 1 Optical micrographs of samples (a) CP-Ti, (b) LC-Steel, (c) SUS316

Table 3 0.2% proof stress (0.2%PS), tensile stress (TS), uniform elongation (U-EL), total elongation (T-EL), r-value, Δr of materials in three directions

Material	Cutting direction	0.2%PS /MPa	TS /MPa	U-EL %	T-EL %	r-value	Δr
CP-Ti	L (0°)	169	296	31	45	2.0	0.5
	D (45°)	188	284	46	59	4.5	
	T (90°)	202	310	5	31	7.9	
	Ave.	187	297	27	45	4.8	–
LC-Steel	L (0°)	138	303	23	43	1.3	0.0
	D (45°)	146	302	23	43	1.5	
	T (90°)	142	303	22	43	1.7	
	Ave.	142	302	23	43	1.5	–
SUS316	L (0°)	265	614	45	54	0.8	-0.1
	D (45°)	263	586	48	58	1.0	
	T (90°)	257	596	52	60	1.0	
	Ave.	262	598	48	57	0.9	–

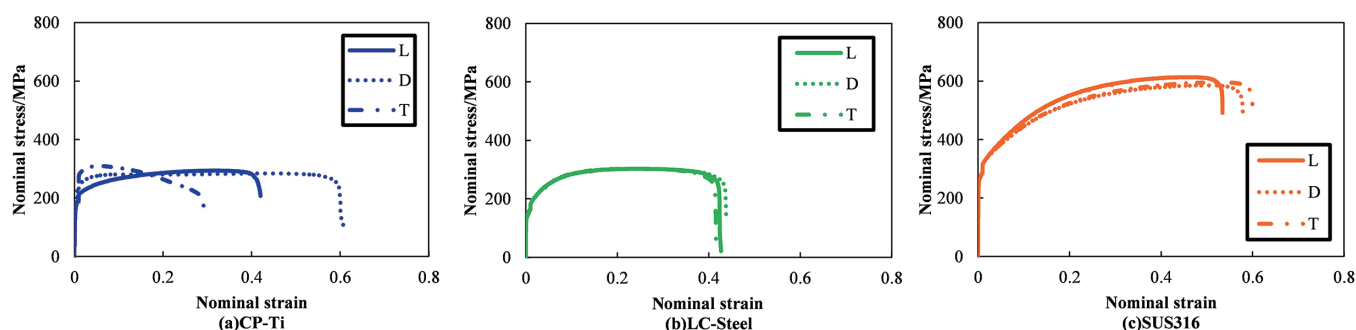


Fig. 2 S-S curve of each material in different tensile directions

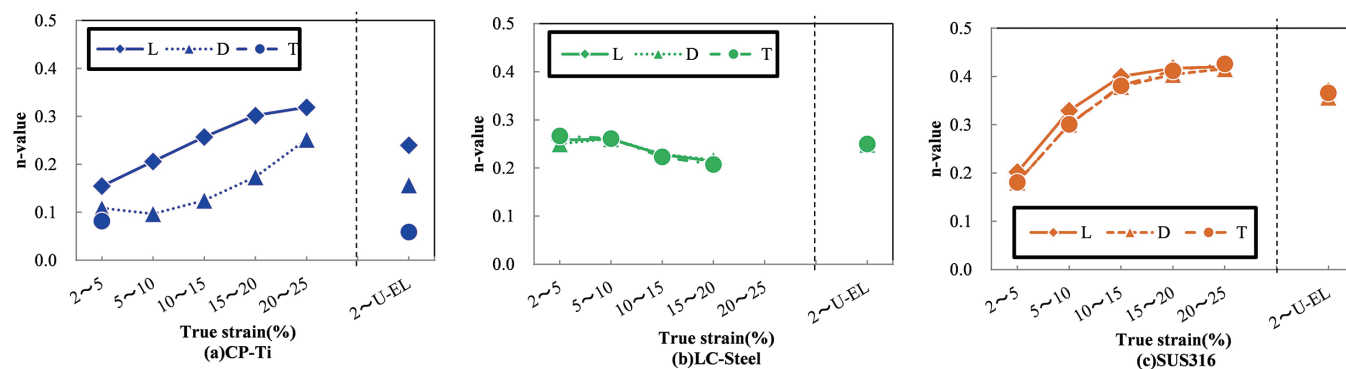


Fig. 3 Effect of strain on the n-value of each material in different tension directions

inafter referred to as the S-S curve). In CP-Ti, anisotropy also exists in work-hardening, and when the S-S curves are compared, the nominal stress of CP-Ti in the L direction and the nominal stress in all directions of LC-Steel and SUS316 tend to increase along with the increase of the nominal strain. In the D direction of CP-Ti, the variation of the nominal stress is small, and in the T direction, the nominal stress becomes highest immediately after the proof stress is measured, and monotonously decreases after that. **Figure 3** shows the effect of strain on the n-value of each material in different tension directions. In the L and D directions of CP-Ti, the n-value increases along with the increase of the true strain. Particularly in the D direction, as the strain becomes higher, the increment of the n-value becomes larger, and is considered to be a factor of the large uniform elongation. Since the uniform elongation of CP-Ti in the T

direction is small, the dependence of the n-value on strain is unknown. On the other hand, the dependence of the n-value of LC-Steel on strain is small, and the n-value of SUS316 increases along with strain like in the L and D directions of CP-Ti. As described above, since the n-value fluctuates depending on the tensile direction and/or strain, it is not possible to make a general comparison for each material. However, when the average n-value of the uniform elongation in the range above 2% elongation is compared, it increases in the order of: T direction of CP-Ti < D direction of CP-Ti < L direction of CP-Ti ≈ LC-Steel < SUS316.

3.2 Hemi spherical punch stretching test and preparation of FLD

Using various size rectangular blanks, the hemi spherical punch stretching test was conducted, and the limiting dome height was

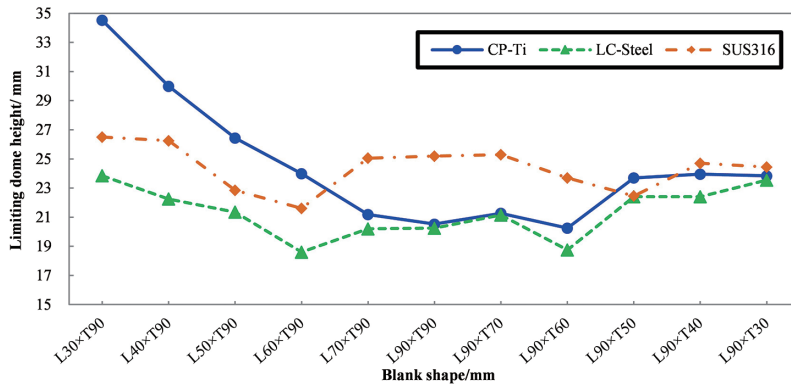


Fig. 4 Effect of blank shape on limiting dome height of each material

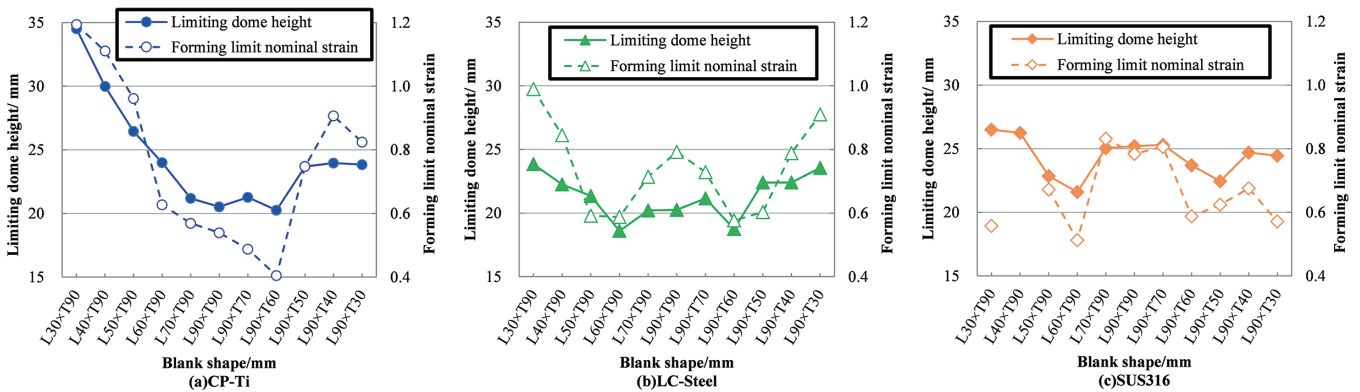


Fig. 5 Effects of blank shape on limiting dome height and forming limit nominal strain of each material

measured. **Figure 4** shows the comparison of the limiting dome height pursuant to the blank shape. Quite adversely to the trend of the anisotropy of the total elongation, the limiting dome height of CP-Ti becomes L (right side in the figure) < T (left side in the figure). When the limiting dome height is compared according to the material, the result becomes: in the range from L30×T90 to L60×T90, LC-Steel<SUS316<CP-Ti, in the range from L70×T90 to L90×T60, LC-Steel≤CP-Ti<SUS316, and in the range from L90×T50 to L90×T30, LC-Steel≈CP-Ti≈SUS316. The limiting dome height of CP-Ti is equal to or higher than that of LC-Steel in any blank shape, and exceeds that of SUS316 depending on the blank shape.

The n-value and the maximum main strain at the fractured part (hereinafter referred to as the forming limit strain) contribute to the limiting dome height.⁵⁾ Therefore, the forming limit strain of the forming test piece was measured, and the relationship with the limiting dome height was investigated. **Figure 5** shows for each blank shape the limiting dome height and the forming limit strain converted to the nominal strain (hereinafter referred to as the forming limit strain (nominal)). Although not in complete agreement as the n-value affects the limiting dome height as well, in any material, the transitions of the limiting dome height and the forming limit nominal strain are of a similar pattern. In the T direction of CP-Ti, the n-value is small. However, the forming limit strain (nominal) is large. Therefore, it is considered that the limiting dome height increases due to the effect of the higher forming limit strain. The forming limit strains (nominal) of the short axis of SUS316 L30×T90 and L90×T30 blanks are small. It is considered that, as shown in **Fig. 6**, a crack developed at the edge of the blank due to the effect of the re-



Fig. 6 Broken part of SUS316 (L30×T90 mm)

straint of the blank holder, and propagated to fracture.

The forming limit strain in the vicinity of the fracture part of the tensile test strain and of the hemi spherical punch stretching test pieces was measured, and an FLD was developed. **Figure 7** shows the FLD of the respective material. The strain mode of the hemi spherical punch stretching test per blank shape is: equibiaxial strain in L90×T90 mm, and plane strain in the rectangular form having 60 mm short axis. Further, although equibiaxial strain deformation was targeted in the LC-Steel L90×T90 mm blank, fracture occurred with a strain mode between the equibiaxial mode and plane mode. Therefore, for the value of the equibiaxial forming limit strain, the value of the fracture part of the hydraulic bulge test piece was used. The CP-Ti forming limit strain differs depending on the direction of the main strain. The value in the L direction is smaller than the one in the T direction and particularly low where the equibiaxial strain changes to the plane strain in the L-direction. In the case that a local

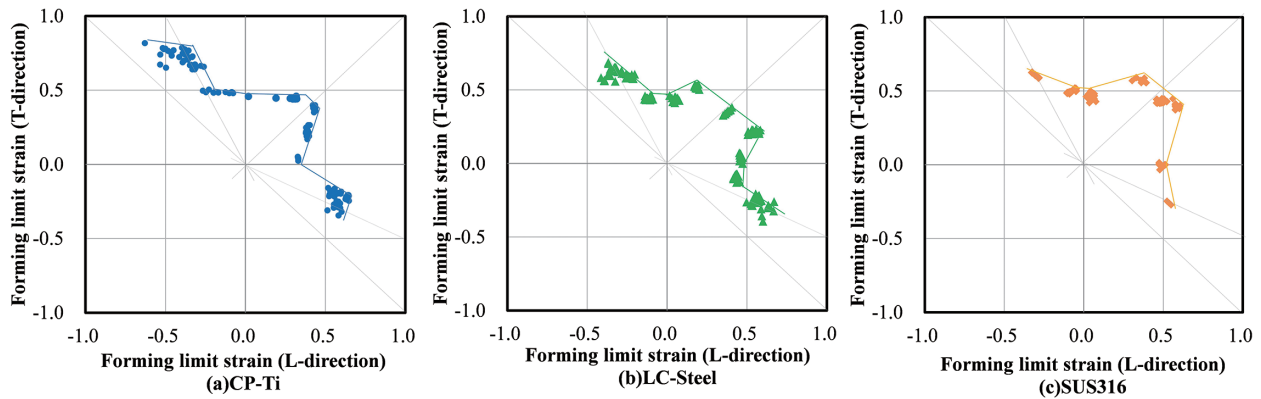


Fig. 7 Forming limit diagram of each material

deformation under this strain mode situation is exerted like for instance in press-forming, precaution must be taken to prevent sudden fracture. Comparing the forming limit strain of each material, in the first quadrant wherein the tension-tension deformation takes place, in the range where the main strain shifts from the equibiaxial strain to the T-direction, the order of the strain is: CP-Ti≈LC-Steel<SUS 316, and in the range wherein the main strain is in the L-direction, the order is: CP-Ti<LC-Steel<SUS310. In the second quadrant having the main strain in the T-direction with the tension-compression deformation, the order is: SUS316<LC-Steel<CP-Ti, and in the fourth quadrant having the main strain in the L-direction with the tension-compression deformation, the order is: SUS316<LC-Steel≈CP-Ti.

3.3 Cylindrical cup drawing test

Figure 8 shows the deep drawing test pieces. The maximum diameters of the deep-drawable blanks are: φ104 mm of CP-Ti (LDR 2.6), φ92 mm of LC-Steel (LDR 2.3), and φ88 mm of SUS316 (LDR 2.2). Figure 9 shows the schematic drawing of the cylindrical cup drawing.⁴⁾ The drawability becomes higher when the fracture load Pa at the punch shoulder (at point a: tension-tension deformation) is higher, and the load Pb (at point b: tension-compression deformation) is smaller to allow the flow of the flange.⁴⁾ The higher the r-value, the larger LDR.⁵⁾ In this test also, LDR grew higher in the order of the increase of the mean r-values of the materials. The maximum stress σ_{pa} produced at the punch shoulder during the cylindrical cup drawing (hereinafter referred to as the shoulder maximum stress) is defined by Expression (2).

$$\sigma_{pa} = \frac{Pa_{max}}{D \cdot t} \quad (2)$$

where, Pa_{max} is the maximum load during the deep-drawing, D is the punch diameter, and t is the initial sheet thickness. Figure 10 shows the effect of the blank diameter on the shoulder maximum stress. To add, the × mark in the figure denotes the fracture at the punch shoulder, and the maximum stress at the punch shoulder at × becomes the fracture stress at the punch shoulder. Although the transitions of the punch shoulder maximum stress of CP-Ti and LC-Steel are the same, differently from the approximate 410 MPa shoulder fracture stress of LC-Steel, the value of CP-Ti is about 480 MPa, far exceeding that of LC-Steel. Considering that the material strength is almost the same judging from the tensile strengths in the L, D, and T directions, the increase in the shoulder fracture stress is considered to greatly contribute to the higher CP-Ti drawability.

In the deep-drawing forming, the ear has a close relation to the anisotropy of the r-value, and a large ear was developed in the CP-

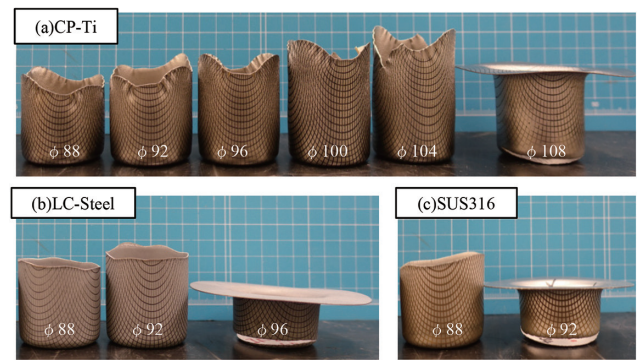


Fig. 8 Deep drawing test piece of each material

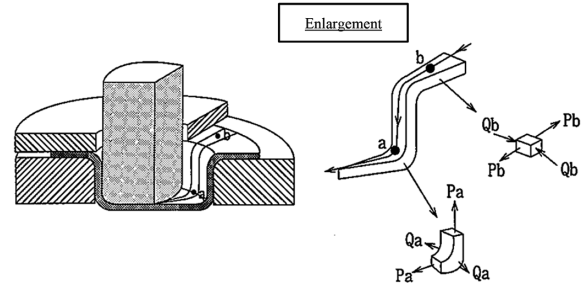


Fig. 9 Schematic of deep drawing test⁴⁾

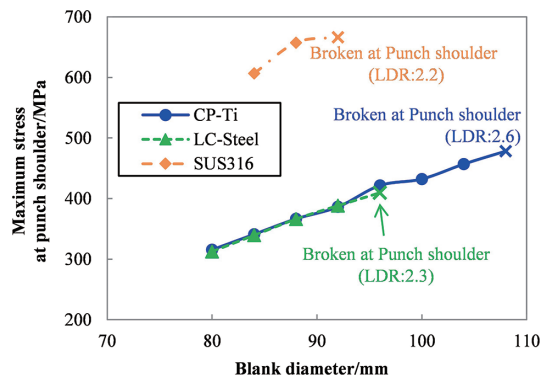


Fig. 10 Effect of blank shape on maximum stress at punch shoulder of each material

Ti drawing. The direction of the formation of the ear is arranged by the in-plane Δr anisotropy.²⁾ For example, when $r_L \approx r_T \neq r_D$ and Δr is positive, the r-values in the L and T directions become higher than

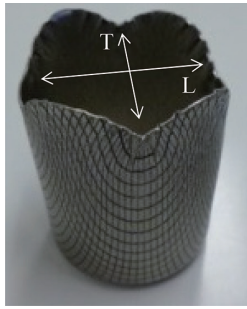


Fig. 11 Deep drawing test piece of CP-Ti ($\phi 96$ mm)

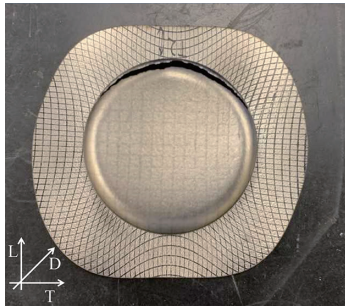


Fig. 12 Flange shape of CP-Ti ($\phi 108$ mm; broken at punch shoulder)

those in the D direction. As a result, the tension-compression deformation is promoted in the direction of the flange, and ears are formed. In the case of the negative Δr , the ear is formed near the D direction according to a similar concept. As Table 3 shows, Δr of CP-Ti is positive 0.5, and as Fig. 11 shows, the ear of CP-Ti is formed near the D direction. However, since the r-value of titanium is arranged in the order of $L < D < T$, and the respective difference is large, the deformation is considered to have been produced based on a mechanism different from the above Δr concept. Figure 12 shows the shape of the flange of the $\phi 108$ mm CP-Ti blank that fractured at the shoulder during deep-drawing. The flange pattern is of the $\square 2$ mm grid marking that had been provided on the blank beforehand. From the curvature of the grid, the tension-compression deformation in the T direction is found to be small with respect to the one in the L direction. The CP-Ti proof stress of 0.2% becomes larger in the order of the $L < D < T$ direction, the deformation in the T direction is suppressed, and to make up for the deformation in the T direction, large deformation is considered to have occurred in the L and D directions. As, at this time, the r-value in the L direction is smaller than the one in the D direction, the deformation in the D direction became relatively larger, and the flange has become square-shaped having a corner in the D direction. As a result, ears have been formed in the D direction having long diagonal lines.

4. Forming Simulation

4.1 Press forming simulation of titanium material

The titanium material for consumer products is used particularly for the press-formed case bodies of IT-related (information technology related) equipment. As mentioned already, working has been considered difficult due to the characteristics of the titanium material with respect to the work-hardening anisotropy and plasticity anisotropy which are greatly different from those of steel.

Then, Nippon Steel Corporation, taking into consideration these characteristics, is in the process of developing an analysis technolo-

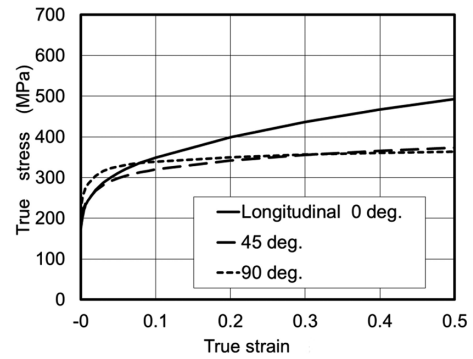


Fig. 13 Anisotropic work-hardening of pure titanium

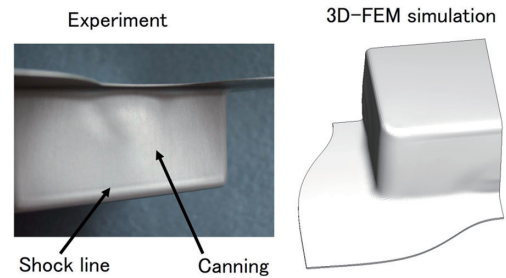


Fig. 14 Forming shape of square rectangular cup drawing

gy that also enables the consideration of the stress in the thickness-direction by using the three-dimensional solid element. To enhance the titanium forming simulation technology, it is necessary to develop and apply a material constitutive law that can simulate the deformation of the titanium material with higher accuracy.

4.2 Simulation method of titanium material

Besides exhibiting plasticity anisotropy having a large r-value, as Fig. 13 shows, the titanium material has the work-hardening anisotropy, having a different stress-strain curve in each direction of tension, and exhibits a deformation behavior different from that of steel. Furthermore, for the analysis that intends to lower the shock line, consideration of the stress in the thickness direction is required.⁶⁾

In this simulation model, for the analysis, the elastoplastic finite element analysis method employing a three dimensional solid element was used, being approximated by the secondary yield function of Hill's quadratic orthotropic yield function of Expression (3).

$$a_1(\sigma_y - \sigma_z)^2 + a_2(\sigma_z - \sigma_x)^2 + a_3(\sigma_x - \sigma_y)^2 + a_4\tau_{yz}^2 + a_5\tau_{xz}^2 + a_6\tau_{xy}^2 = \bar{\sigma}^2 \quad (3)$$

In addition, the work-hardening anisotropy was approximated by the method of taking into consideration the direction of the element inflow.

4.3 Analysis result

This time, by using the pure titanium as shown in Fig. 13, a rectangular cup drawing test was conducted with a $\square 70$ mm punch, and the simulation result was compared with that of the experiment. The blank size was $\square 140$ mm, sheet thickness was 0.5 mm, and the blank holding load was 9.8 kN. A lubricant was used, and the friction coefficient condition of $\mu = 0.05$ was provided. Figure 14 shows the comparison of the state of forming obtained by the simulation and the experiment. From the analysis, the shape forming irregularity such as the canning and the shock line that occur in the experiment is found to be simulated. With the help of this simulation, the study such as setting of the optimum die-clearance accompanying

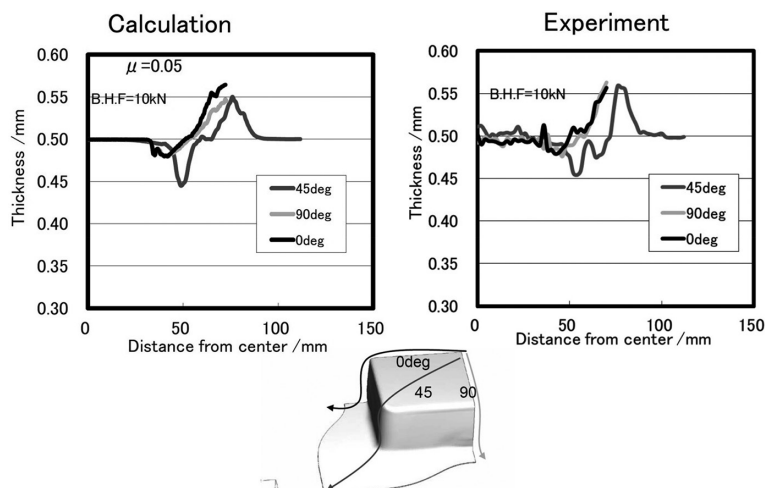


Fig. 15 Thickness distribution of square rectangular cup drawing (H=30 mm)

ironing is enabled in advance.

Figure 15 shows the comparison of the sheet thickness distribution, which shows relatively good agreement. Further expected is the enhancement of the analysis accuracy by applying the element and/or the mesh division appropriate for the higher order curved yield surface and the deformation mode of the finite element method.

4.4 Future prospects

Based on the above content, Nippon Steel is developing a constitutive law that takes into consideration the anisotropic work-hardening, specific to titanium material, wherein the stress-strain relationship differs depending on the direction of the tension of material. By inputting to the constitutive law the actual parameter-values of the stress-strain relation and the r -value obtained from the actual tensile test in the respective direction, and by calculating the stress-strain relation and the r -value by the constitutive law, it is confirmed that the anisotropic work-hardening and plasticity anisotropy can be reproduced relatively accurately. Hereafter we aim to propose solutions to users by developing into practical use the forming and processing simulation technologies.

5. Conclusion

- Titanium has a large anisotropy with respect to the rolling direction (hereinafter referred to as the L direction), the transverse direction (hereinafter referred to as the T direction), and the 45 degree angle direction (hereinafter referred to as the D direction). The 0.2% proof stress increases in the order of: $L < D < T$ direction, and regarding the tensile strength, the order is: $D < L < T$ direction. Furthermore, the r -value increases in the order of: $L < D < T$, and the value in the T direction is as remarkably high as 7.9.
- The order of the uniform elongation of CP-Ti is $T < L < D$ in terms of direction, however, the average n -value is in the order of $T < D < L$, and neither agree with each other. The n -value of CP-Ti increases along with the strain, and it is considered that, in the D direction, the increase of the n -value becomes larger in the higher strain region.
- As the average values of L, D, and T of each material are compared, the order of the total elongation and the tensile strength is: $CP\text{-}Ti \approx LC\text{-}Steel < SUS316$, while the order of the r -value is $SUS316 < LC\text{-}Steel < CP\text{-}Ti$.
- With respect to the limiting dome height of the hemi spherical punch stretching test using various rectangular shaped blanks, in any blank shape, $LC\text{-}Steel \leq CP\text{-}Ti$, and depending on the blank shape, CP-Ti exceeds SUS316. In the T-direction of CP-Ti, although the n -value is small, as the forming limit strain is high, the dome height is good.
- As for the order of the forming limit strain, in the first quadrant (tension-tension), $CP\text{-}Ti \approx LC\text{-}Steel < SUS316$, in the second quadrant (tension in the T direction-compression in the L direction), $SUS316 < LC\text{-}Steel < CP\text{-}Ti$, and in the fourth quadrant (tension in the L direction-compression in the T direction), $SUS316 < LC\text{-}Steel \approx CP\text{-}Ti$.
- As for CP-Ti, the forming limit strain is low where the equibiaxial strain changes to the plane strain in the L direction, and sudden fracture may occur due to the local change of the said strain mode.
- In the cylindrical cup drawing test, LDR is 2.2 for SUS316, 2.3 for LC-Steel, and 2.6 for CP-Ti being the best. However, in CP-Ti, different from the direction predicted by Δr , a large ear was developed in the D direction.
- In the T direction, although the r -value is highest, the proof strength is high, and it is difficult for the deformation to occur, a concave shape is formed, and the strain is concentrated in the D direction having the second largest r -value, and therefore, earing is considered to have occurred.
- Titanium square rectangular cup drawing forming simulation was conducted by using Hill's secondary yield function of the orthogonal anisotropy, the result of which was compared with the experimental result. From the comparison of the shape profile, although a certain difference was recognized in the flow of the material, the thickness distribution had good agreement in both.
- Currently, a material constitutive law is being developed, taking into consideration the work-hardening anisotropy that occurs specifically in titanium material, wherein the stress-strain relation differs depending on the direction of tension. Hereafter, we intend to put into practical use the forming and processing simulation technologies, and the evolution of the proposal of solutions to users.

References

- 1) Yamade, Y. et al.: J. Jpn. Inst. Light Met. 67 (4), 126 (2017)
- 2) Ishiki, M. et al.: Trans. Jpn. Soc. Mech. Eng. Series A. 75 (752), 95 (2009)
- 3) Ohwue, T. et al.: Trans. Jpn. Soc. Mech. Eng. Series A. 79 (801), 79 (2013)
- 4) Usuda, M.: Nippon Steel Technical Report. (85), 24 (2002)
- 5) Yoshida, T.: Bull. Iron Steel Inst. Jpn. 23, 20 (2018)
- 6) Itami, Y.: CAMP-ISIJ. 20 (6), 1403 (2007)



Ryotaro MIYOSHI
Researcher
Titanium & Stainless-steel Research Dept.
Materials Reliability Research Lab.
Steel Research Laboratories
20-1 Shintomi, Futtsu City, Chiba Pref. 293-8511



Yoshiaki ITAMI
Specialized Senior Manager, Dr.Eng
Material Properties Evaluation Div.
Futtsu Unit
Nippon Steel Technology Co., Ltd.